

The phases of isospin asymmetric matter in the two flavor NJL model

S. Lawley,^a ^{b*} W. Bentz^c and A. W. Thomas^b

^aSpecial Research Centre for the Subatomic Structure of Matter,
University of Adelaide, Adelaide SA 5005, Australia

^bJefferson Lab, 12000 Jefferson Avenue, Newport News,
VA 23606, U.S.A.

^cDepartment of Physics, School of Science, Tokai University
Hiratsuka-shi, Kanagawa 259-1292, Japan

We investigate the phase diagram of isospin asymmetric matter at $T=0$ in the two flavor Nambu-Jona-Lasinio model. Our approach describes the single nucleon as a confined quark-diquark state, the saturation properties of nuclear matter at normal densities, and the phase transition to normal or color superconducting quark matter at higher densities. The resulting equation of state of charge neutral matter and the structure of compact stars are discussed.

PACS numbers: 12.39.Fe; 12.39.Ki; 21.65.+f; 97.60.Jd

Keywords: Effective quark theories, Diquark condensation, Phase transitions, Compact stars

1. Introduction

The Nambu-Jona-Lasinio (NJL) model [1] is an effective theory of QCD at intermediate energies where pointlike interactions between quarks replace the full gluon mediated description of quark interactions. The model has been widely used to study cold dense quark matter (QM) [2], because in this region of the QCD phase diagram the explicit gluonic effects are expected to be minor. Furthermore, recent developments of the NJL model have shown the possibility of a realistic description of single nucleons and stable nuclear matter (NM) [3]. Hadronization techniques [4] in principle enable us to study both NM and QM within the framework of a single model, which also accounts for the internal quark structure of the free nucleon [5]. The purpose of this letter is to investigate the phase diagram of this model, extending the work of ref. [4] to the case of isospin asymmetric matter, and to present results for the equation of state (EOS) of charge neutral matter and the structure of compact stars [6].

Many recent theoretical studies have suggested that matter at high densities and low temperatures is in the color superconducting quark matter (SQM) phase [7]. The number of flavors present will depend on the effective quark masses in QM. In particular the behavior of the strange quark mass at high density, which is not well known, plays a critical role in determining the structure of the favored QM phase [8]. In NJL-type models, the strange quark turns out to be heavy enough to favor a transition to the 2-flavor color SQM state [2], whereas the 3-flavor state occurs at still higher densities. There are many recent investigations on the dependence on the strange quark mass [9,10,11] which tend to support this scenario, provided that the quark pairing interaction is strong enough.

In the present work we also examine the effects of color superconductivity on the phase diagrams and the EOS at high densities. It is a first attempt toward the goal of describing possible mixed NM/SQM phases in one framework. We will use a description which, in normal NM, avoids unphysical thresholds for the decay of the nucleon into quarks, thereby simulating the ef-

*Correspondence to: S.Lawley, E-mail:slawley@jlab.org

fect of confinement [3]. We will show the resulting EOS including mixed phases, and discuss the consequences for compact stars.

We derive both NM and QM phases from the flavor SU(2) NJL-Lagrangian,

$$\begin{aligned} \mathcal{L} = & \bar{\psi}(i\not{\partial} - m)\psi + G_\pi ((\bar{\psi}\psi)^2 - (\bar{\psi}\gamma_5\boldsymbol{\tau}\psi)^2) \\ & - G_\omega (\bar{\psi}\gamma^\mu\psi)^2 - G_\rho (\bar{\psi}\gamma^\mu\boldsymbol{\tau}\psi)^2 \\ & + G_s (\bar{\psi}\gamma_5 C\tau_2\beta^A\bar{\psi}^T)(\psi^T C^{-1}\gamma_5\tau_2\beta^A\psi), \quad (1.1) \end{aligned}$$

where we show only the interaction terms relevant for our discussions¹. Here m is the current quark mass, ψ is the flavor SU(2) quark field, and the coupling constants G_π , G_ω and G_ρ characterize the $q\bar{q}$ interactions in the scalar, pseudoscalar and vector meson channels, while G_s refers to the interaction in the scalar diquark channel.

The model is further specified by a regularization scheme, for which we use the proper-time scheme [14] in this work. It is characterized by an infrared cut-off (Λ_{IR}) in addition to the usual ultraviolet one (Λ_{UV}). In the vacuum, the parameters of the model are determined as follows: We fix $\Lambda_{\text{IR}} = 200$ MeV, and choose Λ_{UV} , m and G_π so as to reproduce $f_\pi = 93$ MeV, $m_\pi = 140$ MeV, and constituent quark mass $M_0 = 400$ MeV via the gap equation at zero density. We will set $M = 0$ in QM because the quark mass is already very small in the region where the transition to QM occurs. We have found that including the effective quark mass in this phase does not change the structure of the phase diagrams and has little effect on the EOS.

2. Nuclear matter

The nucleon is constructed as a quark-diquark bound state [5], making use of the scalar diquark interaction term in (1.1) and the Bethe-Salpeter equation to get the scalar diquark mass, M_s . The interaction with the spectator quark is described by the quark exchange (Faddeev) kernel, for which we use a momentum-independent ap-

¹We note that every 4-fermi interaction Lagrangian can be decomposed, as in Eq.(1.1), into various $q\bar{q}$ and qq channels by using Fierz transformations [5]. In the last term of Eq.(1.1), $C = i\gamma_2\gamma_0$ and $\beta^A = \sqrt{3}/2\lambda^A$ ($A = 2, 5, 7$) are the color $\bar{3}$ matrices.

proximation in the finite density calculations reported in this letter. (This corresponds to the ‘‘static approximation’’ of the Faddeev kernel – see Refs.[15,3] for details.) The coupling constant G_s is chosen to reproduce the free nucleon mass, $M_{N0} = 940$ MeV.

In the mean field approximation, the NM phase is characterized by composite neutrons and protons, moving in scalar and vector mean fields. There is also a non-interacting sea of electrons in chemical equilibrium with the nucleons ($\mu_e = \mu_n - \mu_p$, where μ denotes the chemical potential)². The form of the effective potential in the mean field approximation has been derived for symmetric NM in Ref.[4] starting from the quark Lagrangian (1.1) and using the hadronization method. This can be easily extended to the isospin asymmetric case. It has the form

$$V^{(\text{NM})} = V_{\text{vac}} + V_N - \frac{\omega_0^2}{4G_\omega} - \frac{\rho_0^2}{4G_\rho} - \frac{\mu_e^4}{12\pi^2}, \quad (2.1)$$

where

$$\begin{aligned} V_{\text{vac}} = & 12i \int \frac{d^4k}{(2\pi)^4} \ln \frac{k^2 - M^2}{k^2 - M_0^2} \\ & + \frac{(M - m)^2}{4G_\pi} - \frac{(M_0 - m)^2}{4G_\pi} \quad (2.2) \end{aligned}$$

is the vacuum term, and

$$\begin{aligned} V_N = & -2 \sum_{\alpha=p,n} \int \frac{d^3k}{(2\pi)^3} \\ & \Theta(\mu_\alpha^* - E_N(k)) (\mu_\alpha^* - E_N(k)) \quad (2.3) \end{aligned}$$

describes the Fermi motion of nucleons moving in the scalar and vector mean fields. We used $E_N(k) = \sqrt{M_N^2 + k^2}$, where $M_N(M)$ is the nucleon mass in-medium, which is obtained from the pole of the quark-diquark T-matrix. The effective chemical potentials are defined as $\mu_\alpha^* = \mu_\alpha - 3\omega_0 \mp 3\rho_0$ in terms of the mean vector fields $\omega^0 = 2G_\omega \langle \text{NM} | \psi^\dagger \psi | \text{NM} \rangle$ and $\rho^0 = 2G_\rho \langle \text{NM} | \psi^\dagger \tau_3 \psi | \text{NM} \rangle$.

²At some density the components may change, as negatively charged kaon or pion condensates [16] as well as muons replace the electrons and more massive hadron species replace nucleons [17], but here we confine ourselves to the most simple picture.

The constituent quark mass, M , and the mean vector fields in NM are determined by minimizing $V^{(\text{NM})}$ for fixed chemical potentials μ_p and μ_n . The parameter G_ω is fixed by the requirement that the binding energy per nucleon of symmetric NM passes through the empirical saturation point (baryon density $\rho_0 \equiv 0.16 \text{ fm}^{-3}$ and $E_B/A = 15 \text{ MeV}$)³, and the parameter G_ρ is adjusted to the empirical symmetry energy ($a_4 = 32 \text{ MeV}$ at ρ_0). The resulting values of the parameters are shown in the column “NM” of Table 1.

As compared to chiral models for point-nucleons, the important property which leads to saturation of the NM binding energy in this approach is the positive curvature of the function $M_N(M)$, which reflects the internal quark structure of the nucleon and which works efficiently only if there are no unphysical thresholds for the decay of the nucleon into quarks[3]. In our method, these thresholds are avoided by the choice of the proper-time regularization scheme with $\Lambda_{\text{IR}} > 0$ [14].

	NM	QM
m [MeV]	16.93	17.08
G_π [GeV ⁻²]	19.60	19.76
Λ_{UV} [MeV]	638.5	636.7
Λ_{IR} [MeV]	200.0	0
$r_\omega \equiv G_\omega/G_\pi$	0.37	0
$r_\rho \equiv G_\rho/G_\pi$	0.092	0
$r_s \equiv G_s/G_\pi$	0.51	free parameter

Table 1

Parameters used for nuclear matter (left column) and for quark matter (right column). The proper time regularization scheme is used in both cases. Because Λ_{IR} is set to zero in the QM case, the parameters m , G_π and Λ_{UV} differ slightly from the NM values in order to obtain $f_\pi = 93 \text{ MeV}$, $m_\pi = 140 \text{ MeV}$, and $M_0 = 400 \text{ MeV}$.

³We recall from Ref.[3] that G_ω is the only free parameter for NM. With the limited number of parameters in this simple model it is not possible to ensure that the calculated binding energy curve also has a *minimum* at the empirical saturation point. Instead it occurs at $\rho = 0.22 \text{ fm}^{-3}$ and $E_B/A = 17 \text{ MeV}$.

3. Quark matter

The effective potential for QM in the mean field approximation, allowing for the possibility of di-quark condensation, has the form

$$V^{(\text{QM})} = V_{\text{vac}} + V_Q + V_\Delta - \frac{\mu_e^4}{12\pi^2} \quad (3.1)$$

where the vacuum part, V_{vac} , is given by (2.2) and

$$V_Q = -6 \sum_{\alpha=\text{u,d}} \int \frac{d^3k}{(2\pi)^3} \Theta(\mu_\alpha - E_Q(k)) (\mu_\alpha - E_Q(k)) \quad (3.2)$$

describes the Fermi motion of quarks with chemical potentials μ_u and μ_d , and $E_Q(k) = \sqrt{M^2 + k^2}$. The term V_Δ describes the effect of the pairing gap and is given by

$$V_\Delta = 2i \int \frac{d^4k}{(2\pi)^4} \sum_{\alpha=+,-} \left[\ln \frac{k_0^2 - (\epsilon_\alpha + \mu_I)^2}{k_0^2 - (E_\alpha + \mu_I)^2} + \ln \frac{k_0^2 - (\epsilon_\alpha - \mu_I)^2}{k_0^2 - (E_\alpha - \mu_I)^2} \right] + \frac{\Delta^2}{6G_s}, \quad (3.3)$$

where $\epsilon_\pm(k) = \sqrt{(E(k) \pm \mu_q)^2 + \Delta^2}$ and $E_\pm = |E(k) \pm \mu_q|$. Here we used the isoscalar and isovector combinations $\mu_q = (\mu_u + \mu_d)/2$ and $\mu_I = (\mu_u - \mu_d)/2$ ⁴.

A detailed discussion of vector meson poles in Ref.[4] has shown that the vector-type interactions should be set to zero in QM. In addition, we set $\Lambda_{\text{IR}} = 0$, as the infrared cut-off simulates confinement effects which are not appropriate in QM. Also, as stated in the Introduction, we will set $M = 0$ in QM, since the effects of quark mass are small when constructing the phase diagrams and the charge neutral EOS. The resulting parameters are shown in the column “QM” of Table 1. In the main part of this paper we treat G_s as a free parameter in QM to investigate the dependence on the pairing strength, and comment on the important question of consistency with the

⁴We mention that in principle one needs a further chemical potential for color neutrality (μ_s) in QM. However, for the 2-flavor case μ_s turns out to be very small [2,23], and therefore we neglect it here for simplicity.

value derived from the free nucleon mass at the end of Sect.4.

The gap Δ is determined by minimizing the effective potential for fixed quark chemical potentials. In the following discussions, we will distinguish the normal quark matter (NQM) phase, which is characterized by $\Delta = 0$, from the SQM phase ($\Delta > 0$).

4. Results

In order to construct the phase diagram, we compare the effective potentials in the NM, NQM and SQM phases for several fixed chemical potentials for baryon number and isospin (μ_B and μ_I), which are related to the chemical potentials of the particle species by

$$\begin{aligned}\mu_\alpha &= \mu_B \pm \mu_I \quad (\alpha = p, n), \\ \mu_a &= \frac{\mu_B}{3} \pm \mu_I \quad (a = u, d), \\ \mu_e &= -2\mu_I.\end{aligned}\tag{4.1}$$

Fig.1 shows the phase diagrams for several choices of the pairing strength in the SQM phase. The black, dark and light regions indicate the phases with the lowest effective potential, and the \pm indicate the sign of the total charge density⁵. The corresponding plots in the plane of baryon and charge density are shown in Fig.2. The mixed phases appear as white regions in this Figure. The phase boundaries, which are single lines in Fig.1, appear as two lines facing each other in Fig.2. By connecting the corresponding end points on the boundaries by straight lines (dashed lines in Fig.2), we can divide the white region into sections which correspond to mixtures of the two phases facing each other. The $\mu_I = 0$ axes in Fig.1 correspond to the upper-most line running from NM to QM in Fig.2, and because we consider only the case $\mu_I < 0$ the upper left parts of the diagrams in Fig.2 are left empty⁶.

⁵The density of particle $A = p, n, u, d, e$ is obtained as $\rho_A = -\partial V/\partial\mu_A$. In particular, the baryon and charge densities in NM are $\rho_B = \rho_p + \rho_n$, $\rho_c = \rho_p - \rho_n$, and in QM $\rho_B = (\rho_u + \rho_d)/3$, $\rho_c = 2/3\rho_u - 1/3\rho_d - \rho_e$.

⁶In principle we could extend the phase diagrams to the region where $\mu_I < 0$ by admixing positrons instead of

For each case in Fig.1, the charge neutral EOS corresponds to the line separating the positively and negatively charged regions. For example in the first diagram ($r_s = 0$), the charge neutral EOS begins in the pure NM phase, then there is a mixed (+NM/-NQM) phase and finally a pure NQM phase. Each point on the boundary between the NM and NQM phases satisfies the Gibbs conditions, since $P^{(NM)}(\mu_B, \mu_I) = P^{(NQM)}(\mu_B, \mu_I)$. The EOS in the mixed neutral phase is found by using the method of Glendenning [18], that is, the volume fraction of the NM phase is determined by the requirement of charge neutrality as $x^{(NM)} = \rho_c^{(QM)}/(\rho_c^{(QM)} - \rho_c^{(NM)})$, $x^{(QM)} = 1 - x^{(NM)}$. Physically this method implies that the mixed phase begins with charge neutral NM, and then as the charge of NM becomes increasingly positive, regions of negatively charged NQM form, such that the mixed phase remains globally charge neutral⁷. The same sequence of neutral phases can also be seen in the first diagram of Fig.2 by following the horizontal line $\rho_C = 0$.

As we increase the pairing strength in the QM phase, the regions where SQM is the ground state extend. When $r_s = 0.1$ we have a mixed (+NM/-NQM) phase, and then come to a triple point where all three phases meet. This is the same situation as investigated in Ref. [20], and leads to a region of constant pressure in the EOS, where all three phases are mixed. This is illustrated in Fig.2 by the triangular region; that is, when the $\rho_c = 0$ line passes through this region all three phases are present. The volume fraction of SQM begins at zero on the left hand side of the triangle and increases while the volume fraction of NM decreases until it reaches zero on the right hand side of the triangle. The NQM phase occupies the remaining volume fraction, which varies continuously between the boundaries of the triangle. In this region the baryon density is increasing, while the pressure remains constant. However, within compact stars the pressure must always be de-

electrons, but clearly the matter in this part of the phase diagram is always positively charged and is not relevant to the charge neutral EOS.

⁷For such a mixture one may calculate what sizes and shapes are favored for each component [19].

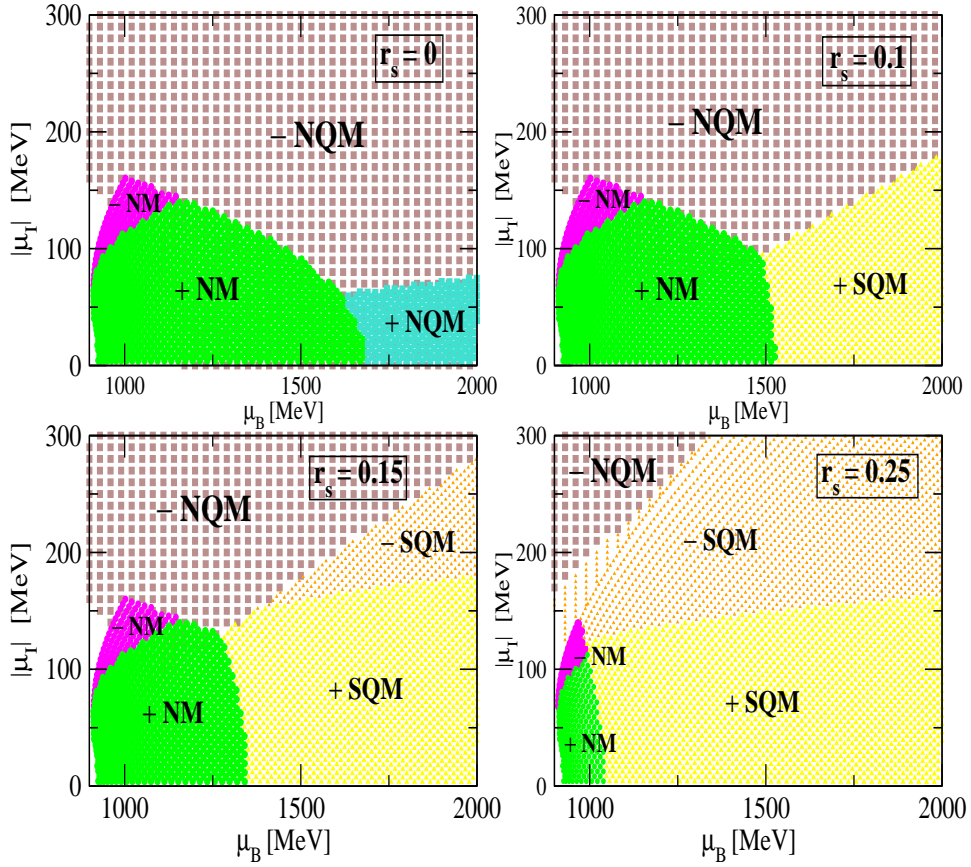


Figure 1. Phase diagrams in the plane of chemical potentials μ_B , μ_I for baryon number and isospin for various choices of r_s . The black, dark and light regions correspond to the NM, NQM and SQM phases, and the \pm indicate the sign of the total charge density including the electrons in chemical equilibrium.

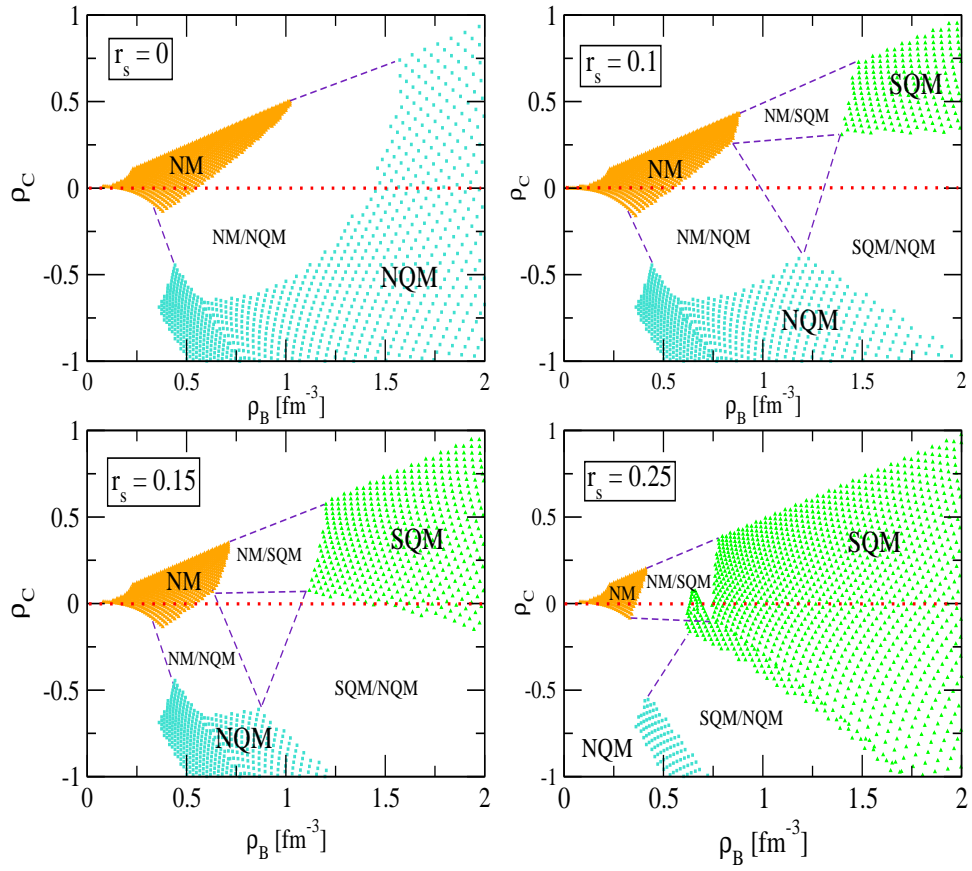


Figure 2. Phase diagrams in the plane of densities ρ_B, ρ_C for baryon number and charge for various choices of r_s . The black, dark and light regions correspond to the NM, NQM and SQM phases, the white regions separated by the dashed lines correspond to the mixture of two phases, and the triangular region for the cases $r_s = 0.1$ and 0.15 involves a mixture of three phases. The upper left regions in each diagram are left empty, because we consider only the case $\mu_I < 0$. The dotted line indicates charge neutrality.

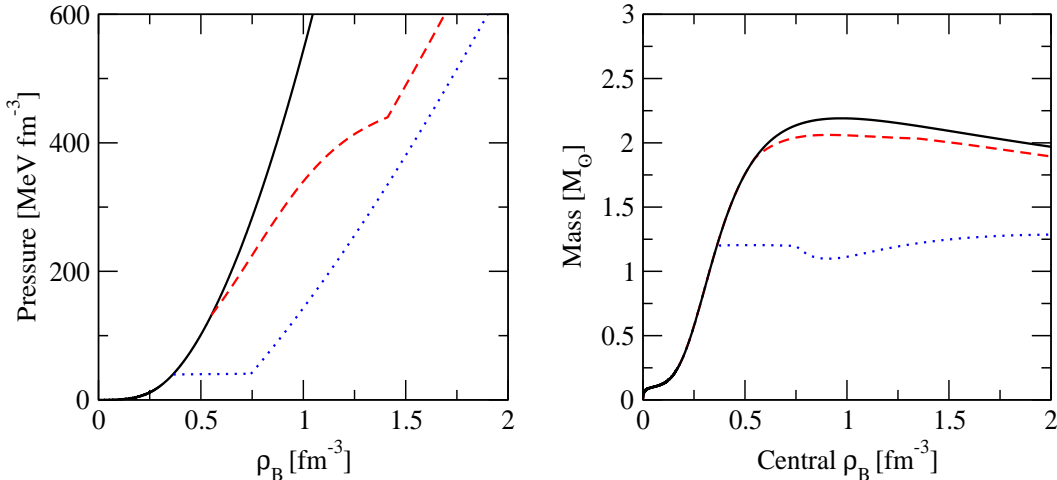


Figure 3. Left figure: Charge neutral EOS (pressure against baryon density) for pure NM (solid line), the transition to NQM (case $r_s = 0$, dashed line), and the transition to SQM (case $r_s = 0.25$, dotted line). Right figure: The corresponding star masses as functions of central density.

creasing as a function of radial position. Thus the three component mixed phase cannot occupy any finite volume within a star and there will be a discontinuity in the star's density profile.

If we further increase the pairing strength to $r_s = 0.15$, a charge neutral SQM state becomes possible. This transition from NM to SQM involves three intermediate mixed phases (NM \rightarrow +NM/-NQM \rightarrow +NM/-NQM/+SQM \rightarrow -NQM/+SQM \rightarrow SQM). Again, the three component mixed phase occurs at the triple point in Fig.1, which corresponds to the triangle in Fig.2. At still larger pairing strengths the NQM phase becomes unfavorable and the EOS involves just NM and SQM. When $r_s = 0.25$ we start with a neutral NM phase, and then enter a (-NM/+SQM) mixed phase before arriving at the neutral SQM phase. In Fig.1 the line along the mixed phase in this case is only very short, which means that the pressure changes in the mixed phase are small. For ($r_s \gtrsim 0.3$) the SQM phase almost completely expels the NM phase, which indicates an upper limit for the pairing strength which is consistent with the findings of Ref.[4] for

the isospin symmetric case.

In Fig.3 we show two examples of the charge neutral EOS, corresponding to the cases $r_s = 0$ and $r_s = 0.25$, and the resulting star sequences obtained by integrating the TOV equation[21]. (The results for the pure NM case are also shown for comparison.) In the first case, the system goes to the NM/NQM mixed phase at a baryon density around $3.4\rho_0$ and the pressure of the mixed phase increases with increasing density. For central densities between $3.4\rho_0$ and $5.6\rho_0$, stable hybrid stars exist with a NM/NQM mixed phase in the center. For example, the maximum mass star has a radius of 11.6 km and the mixed phase is realized within $r = 5.8$ km. In the second case, the transition to the NM/SQM mixed phase occurs at around $2.3\rho_0$, the pressure in the mixed phase is almost constant, and around $4.6\rho_0$ the neutral SQM phase is reached. Stable hybrid stars exist with central densities between $2.3\rho_0$ and $3.4\rho_0$ with a very small region of NM/SQM mixed phase in the center and for central densities between $5.6\rho_0$ and $13.4\rho_0$ stable quark stars may exist, which are composed of SQM in the

central region. For example, the maximum mass star for the case $r_s = 0.25$ has a radius of 8.2 km and the SQM phase is realized within $r = 6.0$ km. These results are qualitatively similar to the ones reported in Ref.[9]. Comparison of two cases shown in Fig.3 indicates that color superconductivity certainly can have a major effect on the EOS. With increasing values of r_s , both the density and the pressure corresponding to the phase transition to QM are significantly reduced, the EOS becomes considerably softer, and the star mass decreases for given central density.

It is interesting to note that for all cases which we studied and where we have a phase transition from neutral NM to neutral SQM (without admixing the NQM phase), the pressure changes only very little in the NM/SQM mixed phase. Then the situation becomes similar to the one where a naive Maxwell construction is applied after imposing the neutrality condition for each phase separately. Including the quark mass in the QM phase does not change our conclusions. In the $r_s = 0.25$ case (which has the lowest transition density) the mass causes only a slight decrease in the pressure ($\Delta P \approx 1\text{MeVfm}^{-3}$) in the region of the mixed phase. This is too small an effect to be seen on the scale of the phase diagram and certainly does not lead to any qualitative changes in our results.

We note that most of the recent calculations on SQM have been performed by using the 3-momentum cut-off scheme and in general the gap is found to be around 100 MeV in the intermediate density region [22]. Our work differs in that we have used the proper time regularization scheme, which leads to larger values of the gap (between 300 and 400 MeV in the relevant density region). However, qualitatively the situation is similar to the cases of strong diquark coupling discussed in Ref.[9,10].

Finally, we would like to come back to the important question of consistency between the values for G_s used for the single nucleon and for the pairing strength in SQM (see Table 1). In this work, we fixed G_s for the single nucleon by fitting the nucleon mass. However, we have to note that there are further attractive contributions to the nucleon mass, most importantly pion exchange

[24,25,26] and contributions of axial vector diquarks [27], which would lead to smaller values of G_s . Indeed, using the expressions given in Ref.[28] for the pion exchange contribution to the nucleon mass, we find that the nucleon mass can be reproduced with $r_s = 0.4(0.25)$, where the two numbers refer to the case without and with further inclusion of axial vector diquarks⁸. Thus the inclusion of pion exchange and axial vector diquarks for the nucleon mass will allow a common value of G_s for the single nucleon and SQM. The details of this calculation will be discussed elsewhere [29].

5. Summary

By applying a flavor SU(2) NJL model to both NM and QM phases, we have studied the phase diagram for isospin asymmetric matter at finite density. We emphasize that the model, and in particular the regularization scheme which we used, describes the single nucleon and the saturation of normal NM, and therefore forms a basis to investigate the EOS at higher densities. We found that, as we vary the pairing strength in QM, several scenarios are possible. The charge neutral EOS may make a transition to NQM or to SQM, via either one, two or three globally charge neutral mixed phases. These transitions begin at small enough densities (2.3 - 3.4 ρ_0) that the QM phase, or at least the mixed phase, may occur inside neutron stars.

ACKNOWLEDGMENTS

The authors wish to thank Dr. David Blaschke for helpful discussions. This work was supported by the Australian Research Council and DOE contract DE-AC05-84ER40150, under which SURA operates Jefferson Lab, and by the Grant in Aid for Scientific Research of the Japanese Ministry of Education, Culture, Sports, Science and Technology, Project No. 16540267.

⁸If axial vector diquarks are included r_s is significantly decreased since there is alternative attraction through this channel. In this case G_a (the axial coupling constant) is fixed using the Fadeev Equation for the Δ and setting $M_\Delta = 1232$ MeV.

REFERENCES

1. Y. Nambu and G. Jona-Lasinio, Phys. Rev. **122** (1960) 345; **124** (1961) 246; see also, U. Vogl and W. Weise, Prog. Part. Nucl. Phys. **27** (1991) 195.
2. For a recent review, see: M. Buballa, Phys. Rep. **407** (2005) 205, and references therein.
3. W. Bentz, A.W. Thomas, Nucl. Phys. **A 696** (2001) 138.
4. W. Bentz, T. Horikawa, N. Ishii and A.W. Thomas, Nucl. Phys. **A 720** (2003) 95.
5. N. Ishii, W. Bentz, K. Yazaki, Nucl. Phys. **A 578** (1995) 617; U. Zückert *et al.* Phys. Rev. **C 55** (1997) 617.
6. N.K. Glendenning, Compact Stars, (Springer, New York, 2000).
7. For reviews on color superconductivity, see: M. Alford, Ann. Rev. Nucl. Part. Sci. **51** (2001) 131; D.H. Rischke, Prog. Part. Nucl. Phys. **52** (2004) 197; K. Rajagopal and F. Wilczek, hep-ph/0011333.
8. M. Alford, Prog. Theor. Phys. Suppl. **153** (2004) 1.
9. D. Blaschke *et al.*, hep-ph/0503194.
10. S. Rüster *et al.*, Phys. Rev. D **72** (2005) 034004; H. Abuki, M. Kitazawa and T. Kunihiro, hep-ph/0412382.
11. K. Fukushima, C. Kouvaris and K. Rajagopal, Phys. Rev. **D 71** (2005) 034002; S.B. Rüster, I.A. Shovkovy and D.H. Rischke, Nucl. Phys. **A 743** (2004) 127.
12. D. Blaschke, D.N. Voskresensky, H. Grigorian, in: Compact Stars (World Scientific, 2004), p. 409 (astro-ph/0403171).
13. F. Weber, Prog. Part. Nucl. Phys. **54** (2005) 193 and references therein.
14. D. Ebert, T. Feldmann and H. Reinhardt, Phys. Lett. **388** (1996) 154; G. Hellstern, R. Alkofer and H. Reinhardt, Nucl. Phys. **A 625** (1997) 697.
15. A. Buck, R. Alkofer and H. Reinhardt, Phys. Lett. **B 286** (1992) 29.
16. H.J. Warringa, D. Boer and J.O. Andersen, Phys. Rev. **D 72** (2005) 014015.
17. G. Baym, in: Compact Stars (World Scientific, 2004), p. 3.
18. N.K. Glendenning, Phys. Rev. **D 46** (1992) 1274.
19. D.G. Ravenhall, C.J. Pethick and J.R. Wilson, Phys. Rev. Lett. **50** (1983) 2066; H. Heiselberg, C.J. Pethick and E.F. Staubo, Phys. Rev. Lett. **70** (1993) 1355.
20. I. Shovkovy, M. Hanauske, M. Huang, Phys. Rev. **D 67** (2003) 103004.
21. J.R. Oppenheimer and G.M. Volkoff, Phys. Rev. **55** (1939) 374.
22. M. Huang, P.F. Zhuang and W.Q. Chao, Phys. Rev. **D 67**, (2003) 065015; H. Grigorian, D. Blaschke and D.N. Aguilera, Phys. Rev. **C 69** (2004) 065802; F. Neumann, M. Buballa, M. Oertel, Nucl. Phys. **A 714** (2003) 481; O. Kiriya, S. Yasui, and H. Toki, Int. J. Mod. Phys. **E 10** (2001) 501.
23. D.N. Aguilera, D. Blaschke and H. Grigorian, Nucl. Phys. **A 757** (2005) 527.
24. M. B. Hecht *et al.*, Phys. Rev. C **65** (2002) 055204.
25. D. B. Leinweber, A. W. Thomas and R. D. Young, Phys. Rev. Lett. **92** (2004) 242002.
26. N. Ishii, Phys. Lett. **B 431** (1998) 1.
27. H. Mineo, W. Bentz, N. Ishii and K. Yazaki, Nucl. Phys. **A 703** (2002) 785.
28. A.W. Thomas and W. Weise, The Structure of the Nucleon, (Wiley-VCH, Berlin, 2001).
29. S. Lawley, W. Bentz and A.W. Thomas, in preparation.